JOURNAL OF PHYSICAL ORGANIC CHEMISTRY
*J. Phys. Org. Chem.* 2005; **18:** 336–346
Published online 5 October 2004 in Wiley InterScience (www.interscience.wiley.com). DOI: 10.1002/poc.869

# A mechanistic viewpoint of the reaction between 1-fluoro-2,6-dinitrobenzene and alicyclic amines in the ethyl acetate–chloroform system

**P. M. Mancini,* G. G. Fortunato and L. R. Vottero**

Departamento de Química, Área Química Orgánica, Facultad de Ingeniería Química, Universidad Nacional del Litoral, Santiago del Estero 2829, (3000) Santa Fe, Argentina

*Received 16 January 2004; revised 14 July 2004; accepted 27 July 2004*

ABSTRACT: A study was made of the influence of temperature on the reactions between 1-fluoro-2,6-dinitrobenzene and each of the secondary amines pyrrolidine, piperidine and homopiperidine (hexahydro-1*H*-azepine), carried out in ethyl acetate–chloroform binary solvent mixtures. It involved the analysis of both global activation parameters and the corresponding Arrhenius plots from the $k_A$ values at three amine concentrations. These values were obtained by carrying out the reactions at 5, 15, 25, 40 and 50 °C over the whole range of chloroform mole fraction. The analysis of Arrhenius lines allowed us to prove the existence of isokinetic relationships, which were used as a diagnostic tool in order to infer a changeover in the nature of the rate-determining transition state as a function of solvent composition. The experimental evidence together with theoretical quantum mechanical calculations suggest that the reactions with the secondary amines explored carried out in pure ethyl acetate and ethyl acetate–chloroform solvent mixture at $X_{CHCl_3} = 0.1$ and in some cases also at $X_{CHCl_3} = 0.3$ proceed via the formation of a six-membered orientated dipolar aggregate in which the specific base–general acid (SB–GA) mechanism may take place. The reactions carried out in the remaining solvent mixtures evolve towards the classical SB–GA mechanism. Copyright © 2004 John Wiley & Sons, Ltd.

*Supplementary electronic material for this paper is available in Wiley Interscience at http://www.interscience.wiley.com/jpages/0894-3230/suppmat/*

KEYWORDS: aromatic nucleophilic substitution; solvent effects; temperature effects; isokinetic relationships; mechanism

## INTRODUCTION

We have recently studied the kinetics of nucleophilic aromatic substitution ($S_NAr$) reactions between 1-fluoro-2,6-dinitrobenzene (2,6-DNFB) and each of the secondary amines homopiperidine (HPIP, hexahydro-1*H*-azepine), pyrrolidine (PYR) and piperidine (PIP) in ethyl acetate–chloroform or acetonitrile and acetonitrile–chloroform binary solvent mixtures.[1] Those studies evaluated the influence of the nucleophile structure and solvent effects on the corresponding reactive systems. It was concluded that the amine structure has a great influence on second-order rate constants, especially on partial rate constants related to the catalyzed step. Theoretical quantum mechanical calculations confirmed that the origin of these results lies in stereoelectronic effects due to the conformational difference between the amino moieties in the $\sigma$ intermediates as they release the nucleofuge. It was also concluded that solvation effects are dominated by non-specific interactions and that the order of incidence of the molecular-microscopic solvent properties on the $k_A$ second-order rate coefficient is dipolarity/polarizability > hydrogen-bond donor ability (HBD) > hydrogen-bond acceptor ability (HBA).

In order to obtain a deeper insight into the kinetic behavior of the reactions between 2,6-DNFB and the secondary alicyclic amines PYR, PIP and HPIP, we analyzed the temperature effect on these reactive systems. In this direction, the reactions were carried out at five temperatures, ethyl acetate (EAc)–cosolvent $CHCl_3$ being the binary solvent system selected. Additionally, from Arrhenius plots obtained for a group of reactions carried out at different temperatures with varying solvent composition, we looked for the existence of an isokinetic relationship. We used this extra-thermodynamic tool in order to infer a possible change in the reaction mechanism of the reactive systems explored.

## RESULTS AND DISCUSSION

The kinetics of the $S_NAr$ reactions between 2,6-DNFB and PYR, PIP and HPIP in the EAc–$CHCl_3$ solvent

**Correspondence to:* P. M. Mancini, Departamento de Química, Área Química Orgánica, Facultad de Ingeniería Química, Universidad Nacional del Litoral, Santiago del Estero 2829, (3000) Santa Fe, Argentina.
E-mail: pmancini@fiqus.unl.edu.ar
*Contract/grant sponsor:* Science and Technology Secretariat, Universidad Nacional del Litoral; *Contract/grant numbers:* 2000-17-151; 2002-21-152; 2002-21-153.

system was determined at 5, 15, 40 and 50 °C. The results corresponding to 25 °C have been reported elsewhere.[1]

Each reaction was explored at different solvent compositions and the influence of the amine concentration was studied in all cases. The reactions were carried out under pseudo-first-order conditions, i.e. with a large excess of the secondary amine. They yielded the expected products in quantitative yield, *N*-(2,6-dinitrophenyl)pyrrolidine, *N*-(2,6-dinitrophenyl)piperidine and *N*-(2,6-dinitrophenyl)homopiperidine, and proved to be first order in the corresponding substrate. Second-order rate constants $k_A$ were calculated by multiplying the observed pseudo-first-order rate constants, $k_\varphi$, by the appropriate amine concentration, $k_A = k_\varphi$ [B].

We assume that the reaction proceeds by the classical two-step mechanism shown in Scheme 1 (where S = substrate, B = amine, ZH = zwitterionic intermediate and P = product). Application of the steady-state approximation for the concentration of ZH, d[ZH]/d[*t*] = 0, yields the following equation for the second-order reaction rate constant $k_A$:

$$k_A = \frac{k_1\left(k_2 + k_3^B[B]\right)}{k_{-1} + k_2 + k_3^B[B]} \quad (1)$$

Three main situations of interest with respect to the reaction shown in Eqn (1) were considered:

(a) $k_{-1} \ll k_2 + k_3{}^B$ [B]. In this case no base catalysis is possible, Eqn (1) simplifies to $k_A = k_1$ and the formation of the zwitterionic intermediate is rate limiting.

(b) $k_{-1} \gg k_2 + k_3{}^B$ [B]. This situation indicates the rapid formation of ZH followed by its rate-determining decomposition. Eqn (1) reduces to

$$k_A = k_1k_2/k_{-1} + k_1k_3/k_{-1}[B] \quad (2)$$

which predicts base catalysis with a linear dependence of $k_A$ on [B].

(c) $k_{-1} \approx k_2 + k_3{}^B$ [B]. In this situation, Eqn (1) indicates that base catalysis is observed with a curvilinear dependence of $k_A$ on [B]. At low [B], the plot of $k_A$ vs [B] should be a straight line which will change to a plateau at high [B], indicating that the formation of ZH is rate limiting.

In polar aprotic solvents, the specific base–general acid (SB–GA) mechanism for the decomposition of ZH has been well established.[2] Scheme 2(a) illustrates the different paths: the formation of ZH, a rapid deprotonation equilibrium of this intermediate, followed by rate-limiting, general acid-catalyzed nucleofuge departure from the anionic $\sigma$ complex $Z^-$, which evolves to products. The derived $k_A$ expression for this mechanism is

$$k_A = \frac{k_1k_2 + k_1k_4^{BH}K_3[B]}{k_{-1} + k_2 + k_4^{BH}K_3[B]} \quad (3)$$

where $k_4{}^{BH}$ is the rate coefficient for acid-catalyzed expulsion of the leaving group and $K_3$ is the deprotonation equilibrium constant.

## Kinetic results

**Reactions with PYR.** Table S1 (Electronic Supplementary Information, ESI; available in Wiley-Interscience) presents the $k_A$ values for the reactions between 2,6-DNFB and all nucleophiles performed at 5, 15, 40 and 50 °C in the explored mixtures. The data in the pure solvents are additionally presented. The corresponding results for the reactions with PYR follow the expected tendency: the $k_A$ values increase as the working temperature increases. As was observed at 25 °C, the kinetic results reveal a satisfactory linear dependence of the rate on amine concentration, showing a null intercept (Table S2 and S3, ESI). As a consequence, the reactions are clearly base catalyzed.

**Reactions with PIP.** As can be appreciated from the data, the $k_A$ values corresponding to the reactions carried out in pure EAc and in the EAc-rich mixtures vary slightly with increasing temperature. Moreover, in some mixtures the values at 40 and 50 °C are smaller than those at 25, 15 and 5 °C.

As in the case of the reactions with PYR, in all instances the second-order rate constant $k_A$ varies linearly

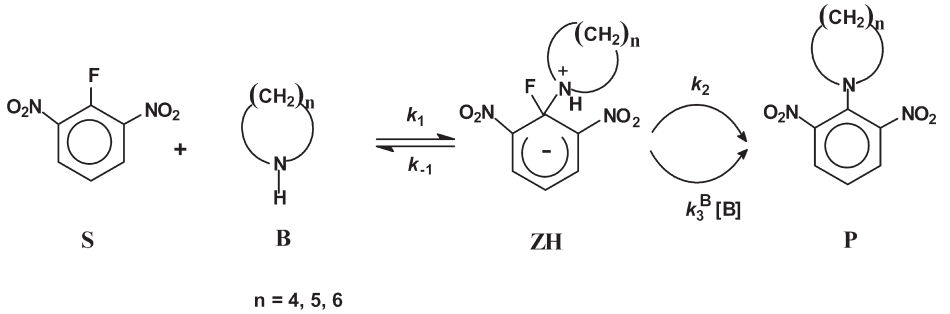


**Scheme 1**

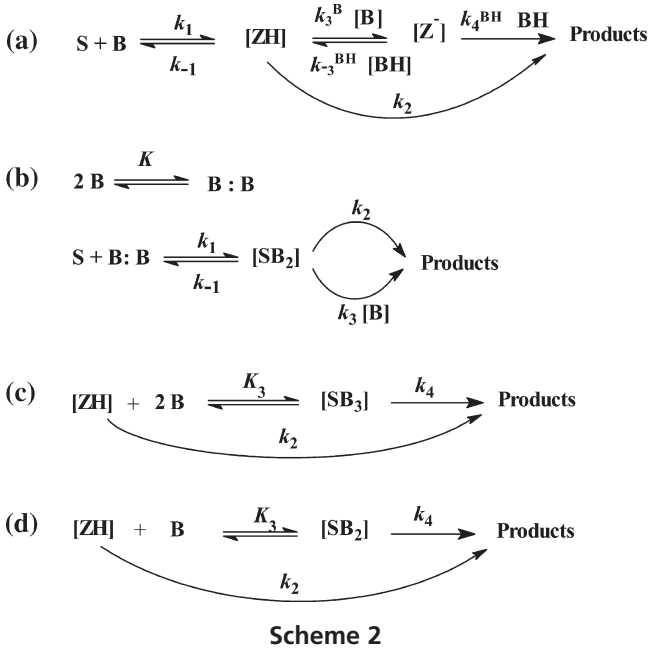


**Scheme 2**

with the amine concentration, exhibiting a null intercept (Tables S4 and S5, ESI).

**Reactions with HPIP.** In pure EAc and in the EAc-rich zone, this reactive system exhibits a kinetic behavior similar to that of the reactions with PIP. For the whole range of temperatures, the $k_A$ values vary linearly with the amine concentration, exhibiting a null intercept in the HBD solvent-poor mixtures (Tables S6 and S7, ESI). The incidence of the base catalysis decreases with the $CHCl_3$ mole fraction.

**Activation parameters.** The global activation parameters $\Delta H^{\#}$, $\Delta S^{\#}$ and $\Delta G^{\#}$ corresponding to reactions with PYR, PIP and HPIP, respectively, are shown in Table 1. Table S8 (ESI) presents the respective Arrhenius parameters. These data were obtained from the $k_A$ values at three different amine concentrations (0.03, 0.07 and 0.15 M) for the reactions of all the reactive systems performed in the solvent mixtures selected.

From the analysis of the respective data, the following tendencies can be observed. In the reactions with all amines, the $\Delta H^{\#}$ and $E_A$ values are significantly low, particularly in the reactions with PIP and HPIP, in which these values are almost zero or negative when they are carried out in pure EAc and in EAc-rich mixtures. The $\Delta H^{\#}$ values vary between 5.243 and 21.17 kJ mol$^{-1}$, −6.041 and 20.38 kJ mol$^{-1}$ and 0.714 and 24.35 kJ mol$^{-1}$ for the reactions with PYR, PIP and HPIP, respectively.

The activation entropies exhibit large negative values. This trend is particularly manifested in mixtures with low cosolvent mole fraction and with PIP and HPIP as nucleophiles. The corresponding values vary from −203.4 to −169.7 J mol$^{-1}$ K$^{-1}$, from −277.8 to −202.6 J mol$^{-1}$ K$^{-1}$ and from −272.9 to −192.6 J mol$^{-1}$ K$^{-1}$ for the reactions with PYR, PIP and HPIP, respectively.

## Isokinetic relationships (*IKR*)

In order to assess the possibility that a specific group of reactions carried out in the different solvent mixtures may be included in an isokinetic relationship (*IKR*), the corresponding Arrhenius lines were plotted. An *IKR* refers to a common point (or small area) of intersection of Arrhenius lines.[3] This would imply that the reactions forming part of the group are similar, constituting a 'series of reactions', and that the reactions go through an equivalent mechanistic pathway. The occurrence or non-occurrence of a common intersection point of the respective lines (even when non-linear behavior is observed[3]) allows us to confirm that possibility. In fact, a common point of intersection of Arrhenius lines is mathematically equivalent to a linear relationship between activation energies and pre-exponential factors or between enthalpy and entropy terms; thus

$$\Delta H^{\#} = \beta \Delta S^{\#} + c \tag{4}$$

where $\beta = T_{iso}$ (isokinetic temperature; K) and $c =$ constant $= \Delta G^{\#}_{\beta}$.

However, this mathematical equivalence does not always hold from a statistical point of view because experimental uncertainties of the *derived* parameters (e.g. $E_A$ and log $A$ or $\Delta H^{\#}$ and $\Delta S^{\#}$) can all too often lead to an artificial linear dependence without a significant meaning.[4] Therefore, a common point of intersection allows one to infer a linear relationship between $\Delta H^{\#}$ and $\Delta S^{\#}$ but the opposite does not hold, i.e. if the corresponding plot renders a linear relationship, this does not necessarily imply that all the reactions constitute a single series of reactions. Krug[5] suggested that the plots of $\Delta H^{\#}$ vs $\Delta G^{\#}_{T\mathrm{hm}}$ or $\Delta G^{\#}_{T\mathrm{hm}}$ vs $\Delta S^{\#}$ were statistically more meaningful ($T_{hm}$ is the harmonic mean of the experimental temperatures). These terms are related by the following equations:

$$\Delta H^{\#} = (1-\gamma)\Delta G^{\#}_{\beta} + \gamma \Delta G^{\#}_{T\mathrm{hm}} \tag{5}$$

$$\Delta G^{\#}_{T\mathrm{hm}} = \Delta G^{\#}_{\beta} + (\beta - T_{\mathrm{hm}})\Delta S^{\#} \tag{6}$$

where $\gamma = 1/(1 - T_{hm}/\beta)$.

Krug based the previous proposal on the fact that the data plotted in the enthalpy–entropy plane appear to display a linear compensation effect that is entirely due to the linear propagation of measurement errors. On the other hand, the data plotted in the $\Delta H^{\#}$–$\Delta G^{\#}_{T\mathrm{hm}}$ plane display structured variations due only to chemical effects because the measurement errors propagate in a random manner into this plane.

**Table 1.** Total activation parameters corresponding to the reactions between 2,6-DNFB and PYR, PIP and HPIP, at [amine] = 0.03, 0.07 and 0.15 M

| | | [Amine] = 0.03 M | | | [Amine] = 0.07 M | | | [Amine] = 0.15 M | | |
|---|---|---|---|---|---|---|---|---|---|---|
| $X_{CoS}$ | Amine | $\Delta H^{\#}$ (kJ mol$^{-1}$) | $\Delta S^{\#}$ (J mol$^{-1}$ K$^{-1}$) | $\Delta G^{\#a}$ (kJ mol$^{-1}$) | $\Delta H^{\#}$ (kJ mol$^{-1}$) | $\Delta S^{\#}$ (J mol$^{-1}$ K$^{-1}$) | $\Delta G^{\#a}$ (kJ mol$^{-1}$) | $\Delta H^{\#}$ (kJ mol$^{-1}$) | $\Delta S^{\#}$ (J mol$^{-1}$ K$^{-1}$) | $\Delta G^{\#a}$ (kJ mol$^{-1}$) |
| 0.0 | PYR | 8.221 ± 0.330 | −197.3 | 67.02 ± 0.33 | 8.329 ± 0.731 | −190.9 ± 69.1 | 65.22 ± 0.73 | 6.009 ± 1.296 | −192.1 ± 154 | 63.25 ± 1.30 |
| | PIP | −4.499 ± 0.269 | −277.8 ± 3.1 | 78.28 ± 0.269 | −6.041 ± 0.480 | −276.0 ± 5.6 | 76.21 ± 0.48 | −3.061 ± 0.103 | −266.2 ± 1.4 | 74.50 ± 0.10 |
| | HPIP | 0.714 ± 0.080 | −272.9 ± 1.0 | 82.04 ± 0.08 | 1.439 ± 0.186 | −262.4 ± 2.5 | 79.63 ± 0.19 | 6.459 ± 0.555 | −239.6 ± 10.6 | 77.86 ± 0.55 |
| 0.1 | PYR | 7.133 ± 0.152 | −203.4 ± 0.9 | 67.75 ± 0.15 | 7.424 ± 0.366 | −195.6 ± 119.6 | 65.71 ± 0.37 | 5.243 ± 0.240 | −196.7 ± 172.9 | 63.86 ± 0.24 |
| | PIP | −1.088 ± 0.058 | −268.3 ± 0.024 | 78.86 ± 0.06 | −3.417 ± 0.109 | −269.3 ± 1.4 | 76.83 ± 0.11 | −4.329 ± 0.035 | −266.2 ± 0.446 | 75.00 ± 0.03 |
| | HPIP | 2.138 ± 0.265 | −268.4 ± 3.3 | 82.12 ± 0.26 | 4.614 ± 0.225 | −251.8 ± 3.5 | 79.65 ± 0.22 | 9.422 ± 0.405 | −299.9 ± 12.6 | 77.93 ± 0.40 |
| 0.3 | PYR | 12.71 ± 0.22 | −185.1 ± 59.1 | 69.09 ± 0.22 | 10.77 ± 0.25 | −188.1 ± 16.3 | 66.82 ± 0.25 | 5.610 ± 0.480 | −199.4 ± 184.2 | 65.03 ± 0.48 |
| | PIP | 3.200 ± 0.240 | −254.9 ± 3.6 | 79.16 ± 0.24 | −0.496 ± 0.086 | −260.8 ± 1.2 | 77.22 ± 0.09 | −4.942 ± 0.237 | −269.4 ± 3.0 | 75.34 ± 0.24 |
| | HPIP | 8.438 ± 0.508 | −248.0 ± 8.4 | 82.34 ± 0.50 | 14.56 ± 1.44 | −218.5 ± 50.6 | 79.70 ± 1.44 | 13.36 ± 1.46 | −217.3 ± 53.8 | 78.11 ± 1.46 |
| 0.5 | PYR | 14.33 ± 1.20 | −185.1 ± 59.1 | 69.49 ± 1.20 | 11.97 ± 0.77 | −186.5 ± 43.4 | 67.55 ± 0.77 | 7.055 ± 0.500 | −196.6 | 65.64 ± 0.50 |
| | PIP | 6.999 ± 0.692 | −243.3 ± 12.3 | 79.50 ± 0.69 | 2.436 ± 0.169 | −251.5 ± 2.6 | 77.38 ± 0.17 | 0.447 ± 0.046 | −252.7 ± 0.7 | 75.75 ± 0.05 |
| | HPIP | 11.18 ± 0.62 | −238.1 ± 12.3 | 82.13 ± 0.62 | 16.84 ± 1.27 | −211.7 ± 64.0 | 79.94 ± 1.27 | 14.73 ± 1.38 | −213.6 ± 62.0 | 78.38 ± 1.38 |
| 0.7 | PYR | 15.59 ± 0.44 | −182.9 ± 18.3 | 70.09 ± 0.44 | 14.09 ± 0.31 | −181.2 ± 11.2 | 68.09 ± 0.31 | 9.643 ± 1.32 | −189.9 ± 108.1 | 66.23 ± 1.32 |
| | PIP | 9.443 ± 0.476 | −236.3 ± 9.7 | 79.77 ± 0.48 | 6.053 ± 0.884 | −240.7 ± 16.5 | 77.78 ± 0.17 | 3.285 ± 0.197 | −244.0 ± 3.4 | 75.99 ± 0.20 |
| | HPIP | 12.69 ± 1.39 | −232.9 ± 30.8 | 82.09 ± 1.39 | 17.71 ± 2.07 | −209.2 ± 125.4 | 80.05 ± 2.07 | 14.55 ± 1.55 | −214.6 ± 65.7 | 78.50 ± 1.55 |
| 0.9 | PYR | 17.13 ± 1.37 | −177.6 ± 46.2 | 70.71 ± 1.37 | 14.63 ± 1.22 | −181.5 ± 45.8 | 68.72 ± 1.22 | 11.49 ± 1.31 | −185.9 ± 69.3 | 66.89 ± 1.31 |
| | PIP | 15.97 ± 1.31 | −215.9 ± 52.1 | 80.31 ± 1.31 | 10.41 ± 0.96 | −227.4 ± 24.7 | 78.17 ± 0.96 | 10.41 ± 1.71 | −221.7 ± 53.9 | 76.48 ± 0.20 |
| | HPIP | 16.32 ± 2.67 | −220.2 ± 83.9 | 81.94 ± 2.67 | 18.57 ± 2.20 | −206.7 ± 169.0 | 80.17 ± 2.20 | 15.79 ± 1.52 | −211.2 ± 79.2 | 78.73 ± 1.52 |
| 1.0 | PYR | 21.17 ± 1.00 | −169.7 ± 20.4 | 71.74 ± 1.00 | 16.74 ± 1.11 | −176.8 ± 31.5 | 69.43 ± 1.11 | 13.87 ± 0.99 | −180.0 ± 33.8 | 67.51 ± 0.99 |
| | PIP | 20.38 ± 0.96 | −202.6 ± 130.6 | 80.75 ± 0.96 | 14.58 ± 0.22 | −214.7 ± 9.2 | 78.56 ± 0.22 | 14.20 ± 2.30 | −209.9 ± 131.7 | 76.56 ± 2.30 |
| | HPIP | 24.35 ± 3.56 | −192.6 ± 79.0 | 81.74 ± 3.56 | 20.83 ± 2.91 | −199.9 | 80.40 ± 2.91 | 18.10 ± 1.72 | −204.7 ± 167.8 | 79.10 ± 1.72 |

[a] At 25 °C.

Additionally, the existence of an *IKR* must be demonstrated statistically. In this direction, Linert proposed a simplified statistical test.[3] When this method yields a positive *IKR* proof, it does so at such significance level that any *IKR* found by this means also holds for the non-simplified method.[4]

In this direction, Arrhenius lines were plotted for the reactions with PYR, PIP and HPIP at three amine concentrations varying the cosolvent molar fraction. The $\Delta H^{\#}$–$\Delta S^{\#}$ and $\Delta G^{\#}_{T\mathrm{hm}}$–$\Delta S^{\#}$ plots are also presented.

**[PYR] groups.** Figure 1 presents the Arrhenius lines belonging to reactions with PYR: [PYR] = 0.03 M group, [PYR] = 0.07 M group and [PYR] = 0.150 M group. $\Delta H^{\#}$–$\Delta S^{\#}$, $\Delta H^{\#}$–$\Delta G^{\#}_{T\mathrm{hm}}$ and $\Delta G^{\#}_{T\mathrm{hm}}$–$\Delta S^{\#}$ plots for each group of reactions are shown in Figs S1, S2 and S3 (ESI), respectively.

The Arrhenius lines clearly yield two intersection points in all cases, indicating in the first instance that the reactions are included in two different groups. The $\Delta H^{\#}$–$\Delta G^{\#}_{T\mathrm{hm}}$ and $\Delta G^{\#}_{T\mathrm{hm}}$–$\Delta S^{\#}$ plots also indicate an equivalent tendency and from the linear treatment of the respective straight lines it was possible to estimate the $\beta$ values (Table 2) according to Eqns (3) and (4). For the [PYR] = 0.03 and 0.07 M groups, the $\Delta H^{\#}$–$\Delta S^{\#}$ plots suggest that all the reactions constitute only one series but the $\Delta H^{\#}$–$\Delta G^{\#}_{T\mathrm{hm}}$ and $\Delta G^{\#}_{T\mathrm{hm}}$–$\Delta S^{\#}$ plots confirm that they are involved in two groups.

Linert's simplified statistical *IKR* analysis was applied to Group 2 for each amine concentration. The respective $T_{\mathrm{iso}}$, $k_{\mathrm{iso}}$ and *F*-distributed values are shown in Table 2. The test allowed us to accept the existence of an *IKR* at the 95% confidence level in all cases.

As a consequence, the reactions can be distributed as Group 1, $X_{\mathrm{CoS}} = 0.0$, 0.1 and Group 2, $X_{\mathrm{CoS}} = 0.1$, 0.3, 0.5, 0.7, 0.9, 1.0. For the reactions corresponding to [PYR] = 0.03 and 0.07 M, that carried out in the solvent $X_{\mathrm{CoS}} = 0.1$ would represent an inflection point. Otherwise, the system corresponding to [PYR] = 0.15 M is distinguished by a break between the two groups.

**[PIP] groups.** Figure 2 presents the Arrhenius lines belonging to the reactions with PIP at the explored amine concentrations. Figures S4, S5 and S6 (ESI) present $\Delta H^{\#}$–$\Delta S^{\#}$, $\Delta H^{\#}$–$\Delta G^{\#}_{T\mathrm{hm}}$ and $\Delta G^{\#}_{T\mathrm{hm}}$–$\Delta S^{\#}$ plots for each group of reactions.

As in the previous groups, the Arrhenius lines yield two intersection points for the three amine concentrations, indicating that the reactions conform to two reaction series. While the $\Delta H^{\#}$–$\Delta S^{\#}$ plot yields a linear relationship, the corresponding $\Delta H^{\#}$–$\Delta G^{\#}_{T\mathrm{hm}}$ and $\Delta G^{\#}_{T\mathrm{hm}}$–$\Delta S^{\#}$ plot reveals that two groups of reactions are involved. Linert's simplified statistical *IKR*-analysis was applied to Group 2 for each amine concentration and to Group 1 for [PIP] = 0.15 M. The respective $T_{\mathrm{iso}}$, $k_{\mathrm{iso}}$, $\beta$ and *F*-distributed values are shown in Table 3. The test allowed us to accept the existence of an *IKR* at the 95% confidence level in all cases.

For the reactions corresponding to [PIP] = 0.03 M and [PIP] = 0.07 M the series are constituted as follows, Group 1: $X_{\mathrm{CoS}} = 0.0$, 0.1 and Group 2: $X_{\mathrm{CoS}} = 0.1$, 0.3, 0.5, 0.7, 0.9, 1.0. The one carried out in solvent $X_{\mathrm{CoS}} = 0.1$ would represent an inflection point between one $T_{\mathrm{iso}}$ and another. The reactions corresponding to [PIP] = 0.15 M are distributed as Group 1: $X_{\mathrm{CoS}} = 0.0$, 0.1, 0.3 and Group 2: $X_{\mathrm{CoS}} = 0.3$, 0.5, 0.7, 0.9, 1.0. As in the previous case, the reaction at $X_{\mathrm{CoS}} = 0.3$ is indicating a change from one series to the other. It must be pointed out that the $T_{\mathrm{iso}}$ (46.7 °C) corresponding to Group 2 is very close to the experimental one (50 °C) which coincides with the fact that the reaction rate is almost constant.

**[HPIP] groups.** Arrhenius lines belonging to the reactions with HPIP at the explored amine concentrations are presented in Figure 3. The $\Delta H^{\#}$–$\Delta S^{\#}$, $\Delta H^{\#}$–$\Delta G^{\#}_{T\mathrm{hm}}$ and

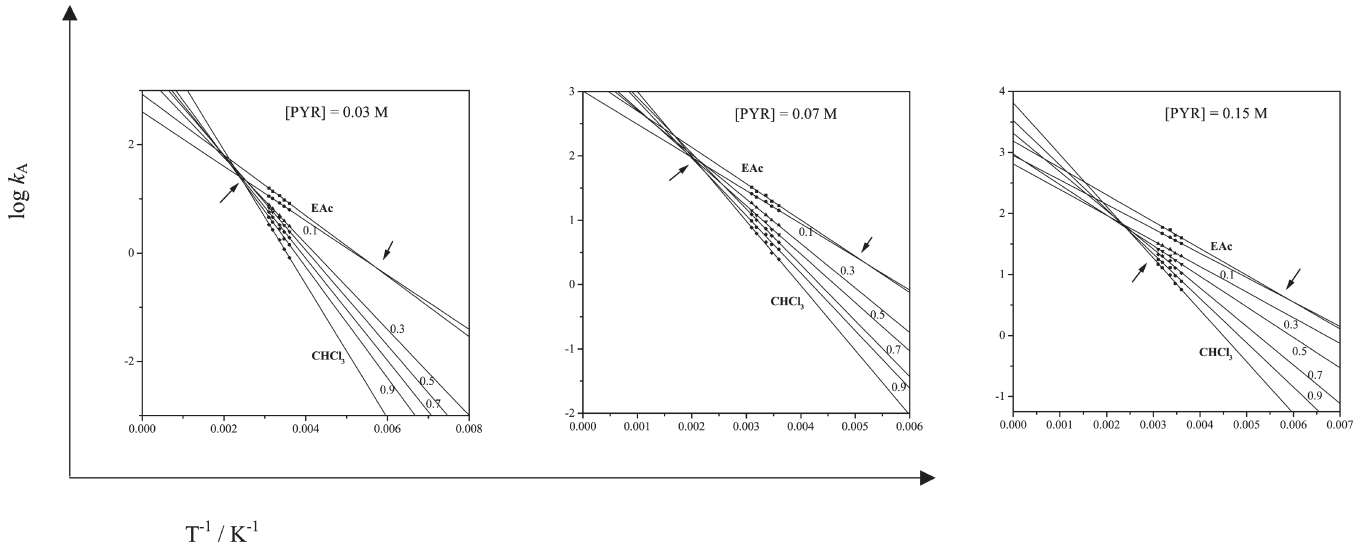


**Figure 1.** Arrhenius lines for [PYR] = 0.03, 0.07 and 0.15 M

 

**Table 2.** $k_{iso}$, $T_{iso}$, $F$ and $\beta$ values corresponding to the reactions with PYR

| [Amine] (M) | Groups: solvent mixtures | $k_{iso}$ ($l\,mol^{-1}\,s^{-1}$) | $T_{iso}$ (K) (°C) | $F_{0.05}(f_1, f_2)$ calculated | $F_{0.05}(f_1, f_2)$ tabulated | $\beta$ (K) | |
|---|---|---|---|---|---|---|---|
| | | | | | | $\Delta G^{\#}_{Thm}$–$\Delta S^{\#}$ | $\Delta H^{\#}$–$\Delta G^{\#}$ |
| 0.03 | Group 1: $X_{CoS} = 0.0, 0.1$ | 0.57 | 175.8 (−97.2) | | | 178.3 | 178.3 |
| | Group 2: $X_{CoS} = 0.1, 0.3, 0.5, 0.7, 0.9, 1.0$ | 26.9 | 423.5 (159.5) | $0.58_{(5,18)}$ | $2.77_{(5,18)}$ | 420.4 ($r = 0.987$) | 423.0 ($r = 0.993$) |
| 0.07 | Group 1: $X_{CoS} = 0.0, 0.1$ | 2.13 | 192.7 (−80.3) | | | 193.7 | 193.3 |
| | Group 2: $X_{CoS} = 0.1, 0.3, 0.5, 0.7, 0.9, 1.0$ | 94.0 | 492.8 (219.8) | $0.59_{(5,18)}$ | $2.77_{(5,18)}$ | 496.4 ($r = 0.980$) | 504.9 ($r = 0.993$) |
| 0.150 | Group 1: $X_{CoS} = 0.0, 0.1$ | 3.62 | 167.7 (−105.3) | | | 165.4 | 165.9 |
| | Group 2: $X_{CoS} = 0.3, 0.5, 0.7, 0.9, 1.0$ | 62.3 | 421.4 (148.4) | $0.065_{(4,15)}$ | $3.06_{(4,15)}$ | 422.0 ($r = 0.993$) | 426.2 ($r = 0.995$) |

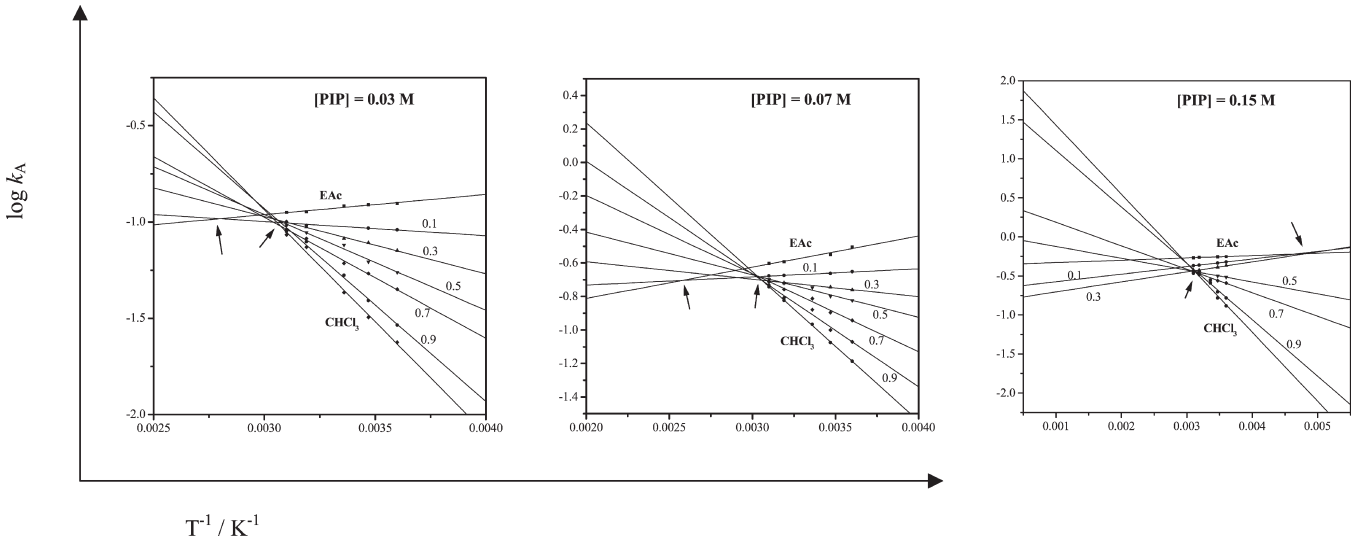


**Figure 2.** Arrhenius lines for [PIP] = 0.03, 0.07 and 0.15 M

**Table 3.** $k_{iso}$, $T_{iso}$, $F$ and $\beta$ values corresponding to the reactions with PIP

| [Amine] (M) | Groups: solvent mixtures | $k_{iso}$ ($l\,mol^{-1}\,s^{-1}$) | $T_{iso}$ (K) (°C) | $F_{0.05}(f_1, f_2)$ calculated | $F_{0.05}(f_1, f_2)$ tabulated | $\beta$ (K) | |
|---|---|---|---|---|---|---|---|
| | | | | | | $\Delta G^{\#}_{Thm}$–$\Delta S^{\#}$ | $\Delta H^{\#}$–$\Delta G^{\#}$ |
| 0.03 | Group 1: $X_{CoS} = 0.0, 0.1$ | 0.104 | 358.9 (85.9) | $0.58_{(5,18)}$ | $2.77_{(5,18)}$ | 359 | 359 |
| | Group 2: $X_{CoS} = 0.1, 0.3, 0.5, 0.7, 0.9, 1.0$ | 0.099 | 326.6 (53.6) | $0.29_{(5,17)}$ | $2.81_{(5,17)}$ | 327 ($r = 0.998$) | 327 ($r = 0.999$) |
| 0.07 | Group 1: $X_{CoS} = 0.0, 0.1$ | 0.197 | 388.0 (115) | | | 390.5 | 390.2 |
| | Group 2: $X_{CoS} = 0.1, 0.3, 0.5,0.7, 0.9, 1.0$ | 0.205 | 328.8 (55.8) | $0.25_{(5,16)}$ | 2.85 (5,16) | 328.9 ($r = 0.997$) | 329.1 ($r = 0.998$) |
| 0.150 | Group 1: $X_{CoS} = 0.0, 0.1, 0.3$ | 0.617 | 207.6 (−68.4) | $0.26_{(2,6)}$ | $5.14_{(2,6)}$ | 206.6 | 206.6 ($r = 0.999$) |
| | Group 2: $X_{CoS} = 0.3, 0.5,0.7, 0.9, 1.0$ | 0.362 | 319.7 (46.7) | $1.56_{(4,12)}$ | $3.26_{(4,12)}$ | 319.1 ($r = 0.990$) | 319.4 ($r = 0.990$) |

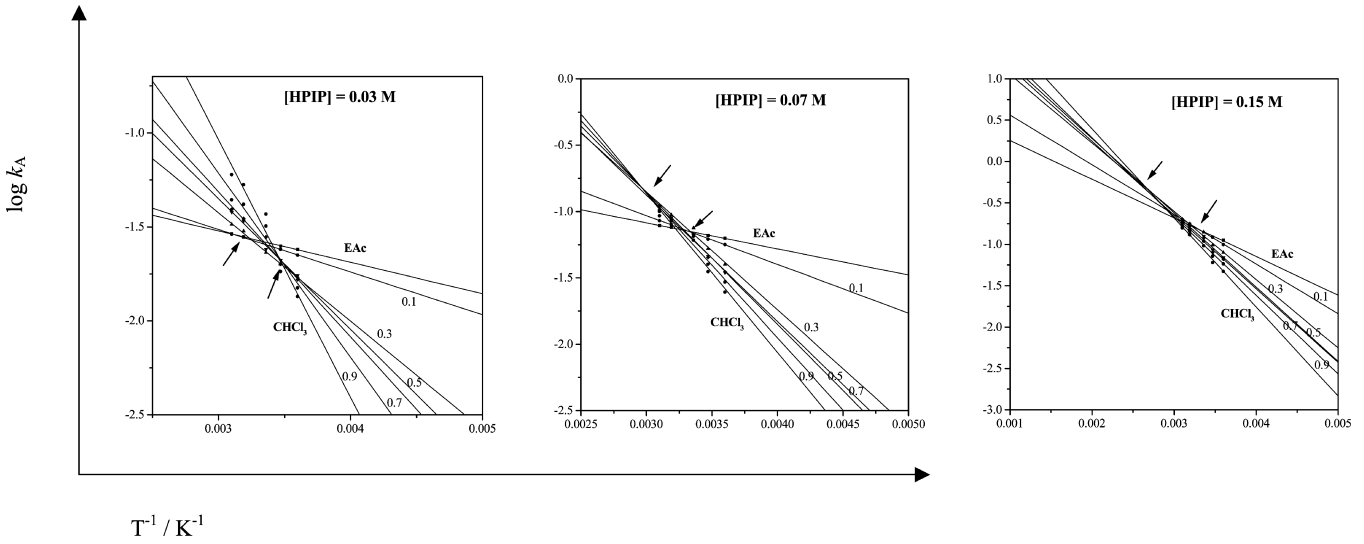


**Figure 3.** Arrhenius lines for [HPIP] = 0.03, 0.07 and 0.15 M

$\Delta G^{\#}_{Thm}$–$\Delta S^{\#}$ plots for the reaction at [HPIP] = 0.15 M are presented in Figure 4. The plots corresponding to the reactions at [HPIP] = 0.03 M and [HPIP] = 0.07 M are presented in Figures S7 and S8 (ESI).

In all cases, Arrhenius plots clearly yield two intersection points indicating the occurrence of two reaction series. This is confirmed by the $\Delta H^{\#}$–$\Delta G^{\#}_{Thm}$ and $\Delta G^{\#}_{Thm}$–$\Delta S^{\#}$ plots and by the statistical test. Table 4 presents $\beta$ values obtained from these plots and $T_{iso}$, $k_{iso}$ and $F$-distributed values graphically obtained from the Arrhenius lines and by means of the respective test. The reactions at [HPIP] = 0.03 M are involved in the following groups: Group 1, $X_{CoS} = 0.0$, 0.1, 0.3 and Group 2, $X_{CoS} = 0.3$, 0.5, 0.7, 0.9, 1.0, the reaction at $X_{CoS} = 0.3$ indicating a change from one series to the other. Reactions of Group 1 exhibit a $T_{iso}$ value (35.7 °C) almost equivalent to the experimental value, indicating that the reaction rate at that temperature is not influenced by the solvent. Group 2 reactions present a $T_{iso}$ value (14.2 °C) which also belongs to the experimental temperature range, with the following consequences: (i) the $k_A$ second-order rate coefficients corresponding to the reactions carried out at 15 °C exhibit little change as the $CHCl_3$ mole fraction increases; (ii) at that temperature, the solvent effect is reversed: the reaction rates at 25, 40 and 50 °C increase with increase in $CHCl_3$ mole fraction whereas those at 5 °C do the opposite.

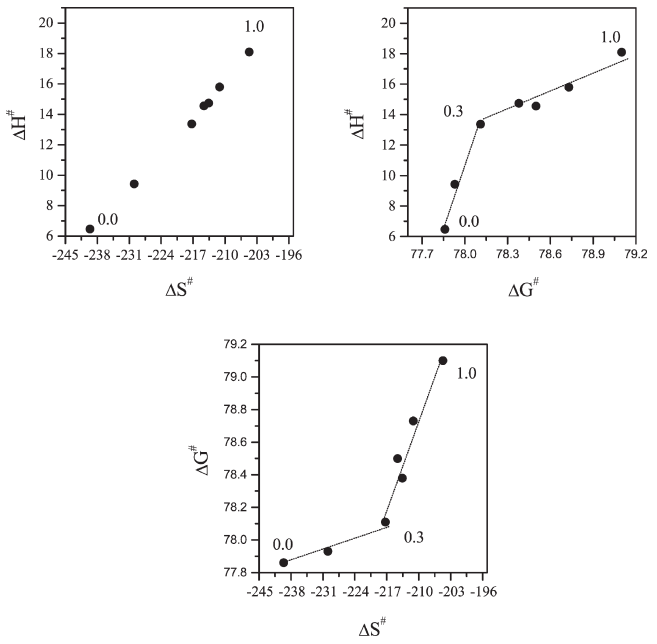


**Figure 4.** $\Delta H^{\#}$–$\Delta S^{\#}$, $\Delta H^{\#}$–$\Delta G^{\#}$ and $\Delta G^{\#}$–$\Delta S^{\#}$ plots for the $k_A$ [HPIP] = 0.15 M group

With respect to the reactions corresponding to [HPIP] = 0.07 and 0.15 M, they are distributed in the same groups as the previous amine concentration: Group 1, $X_{CoS} = 0.0$, 0.1, 0.3 and Group 2, $X_{CoS} = 0.3$, 0.5, 0.7, 0.9, 1.0, the reaction at $X_{CoS} = 0.3$ also indicating a change from one series to the other. The $T_{iso}$ values corresponding to Group 1 from [HPIP] = 0.07 M and 0.15 M belong to the experimental range. For the [HPIP] = 0.07 M group, $T_{iso}$ is ~25 °C so that reaction rates at this temperature are not influenced to a great extent by the change in solvent composition. Otherwise, the reaction rates at 5 and 15 °C decrease with increase in $CHCl_3$ mole fraction whereas the reactions carried out at 40 and 50 °C exhibit an increase in reaction rates. For the [HPIP] = 0.15 M group, $T_{iso}$ is 37 °C. Therefore, it can be observed that below this temperature, reaction rates decrease with increase in $CHCl_3$ mole fraction and above that temperature they do the opposite, although slightly.

The above results suggest the occurrence of a change in the nature of the mechanistic pathway for all the amines explored as a function of solvent composition.

**Table 4.** $k_{iso}$, $T_{iso}$, $F$ and $\beta$ values corresponding to the reactions with HPIP

| [Amine] (M) | Groups: solvent mixtures | $k_{iso}$ (l mol$^{-1}$ s$^{-1}$) | $T_{iso}$ (K) (°C) | $F_{0.05}(f_1, f_2)$ calculated | $F_{0.05}$ ($f_1$, $f_2$) tabulated | $\beta$ (K) | |
|---|---|---|---|---|---|---|---|
| | | | | | | $\Delta G^{\#}_{Thm}$–$\Delta S^{\#}$ | $\Delta H^{\#}$–$\Delta G^{\#}$ |
| 0.03 | Group 1: $X_{CoS} = 0.0, 0.1, 0.3$ | 0.027 | 308.7 (35.7) | $0.34_{(2,6)}$ | $5.14_{(2,6)}$ | 309.7 ($r = 0.996$) | 309.7 ($r = 0.996$) |
| | Group 2: $X_{CoS} = 0.3, 0.5, 0.7, 0.9, 1.0$ | 0.020 | 287.2 (14.2) | $0.03_{(4,15)}$ | $3.06_{(4,15)}$ | 287.8 ($r = 0.973$) | 287.2 ($r = 0.971$) |
| 0.07 | Group 1: $X_{CoS} = 0.0, 0.1, 0.3$ | 0.070 | 299.0 (26) | $1.18_{(2,7)}$ | $4.74_{(2,7)}$ | 298.0 ($r = 0.958$) | 298.0 ($r = 0.958$) |
| | Group 2: $X_{CoS} = 0.3, 0.5, 0.7, 0.9, 1.0$ | 0.150 | 337.8 (64.8) | $0.05_{(4,15)}$ | $3.06_{(4,15)}$ | 337.7 ($r = 0.998$) | 337.8 ($r = 0.999$) |
| 0.150 | Group 1: $X_{CoS} = 0.0, 0.1, 0.3$ | 0.165 | 310.0 (37) | $1.58_{(2,7)}$ | $4.74_{(2,7)}$ | 309.6 ($r = 0.985$) | 309.7 ($r = 0.986$) |
| | Group 2: $X_{CoS} = 0.3, 0.5, 0.7, 0.9, 1.0$ | 0.027 | 308.7 (35.7) | $0.34_{(2,6)}$ | $5.14_{(2,6)}$ | 309.7 ($r = 0.996$) | 309.7 ($r = 0.996$) |

## Mechanistic aspects

In pure EAc and in its richest mixtures, the reactions are highly catalyzed over the whole range of amine concentration at all temperatures and the zwitterionic intermediate decomposition can be considered as the slow step. The reactions are characterized as exhibiting low activation energies and enthalpies and for the reactions with PIP and HPIP they are practically zero and in some cases negative. The reactions are also characterized by large negative entropies of activation. The $k_A$ values remain nearly constant and in some instances they decrease slightly with increasing temperature.

With respect to the above results it can be considered that: (i) total third-order reactions are characterized by low activation energies, large negative entropies of activation and rates exhibiting little change with increasing temperature;[6] (ii) these parameter magnitudes were found in the mechanism involving the formation of EDA-type complexes;[7] (iii) they characterize reactions that are second order in amine, involving a six-membered cyclic transition state with two molecules of amine, with $k_A$ values varying slightly as the reaction temperature is increased;[8,9] (iv) null activation energies, negative $\Delta H^{\#}$ and large negative $\Delta S^{\#}$ were also found in reaction mechanisms third order in amine: dimer mechanism,[10] cyclic transition state involving eight-membered rings.[11] Moreover, in these mechanisms the reaction rates were found to increase slightly with increasing temperature and in some instances reaction rates decrease with increasing temperature.

The dimer nucleophile mechanism was proposed by Nudelman and Palleros.[10] This mechanism exhibits a third-order dependence on the amine involving the attack of the dimer of the nucleophile superimposed on the classical reaction with the monomer. A cyclic intermediate is formed straightforwardly in the addition step through the dimer of the amine. This intermediate is in mobile equilibrium with the classical intermediate and either of them can react to form ultimate products, by spontaneous or base-catalyzed decomposition. A simplified reacting scheme, where only attack of the dimer is considered, is shown in Scheme 2(b). The dimer of the nucleophile (B:B) attacks the substrate, S, forming the intermediate, $SB_2$, and a third molecule of amine assists the decomposition step. The derived expression for $k_A$ in this simplified reacting scheme is

$$k_A = \frac{k_1 k_2 K[B] + k_1 k_3 K[B]^2}{k_{-1} + k_2 + k_3[B]} \quad (7)$$

Plots of $k_A$ vs [B] exhibit an upward curvature and when $k_{-1} \gg k_2 + k_3$ [B] the previous equation can be simplified to

$$k_A/[B] = k_1 k_2 / k_{-1} + k_1 k_3 / k_{-1}[B] \quad (8)$$

which predicts a linear dependence of $k_A$/[B] vs [B]. When $k_{-1} \approx k_2 + k_3$ [B], at high [B], Eqn (7) can be transformed into the equation $k_A/[B] = k_1 K$, which is responsible for the plateau observed in some cases in the plot of $k_A$/[B] vs [B].[10]

In reference to our reactive systems, reactions with all the nucleophiles for the explored amine concentrations do not exhibit the characteristic upward curvature over the whole range of temperatures. Otherwise, the plots of $k_A$/[B] vs [B] do not afford straight lines.

The cyclic transition state involving eight-membered rings mechanism was proposed by Banjoko and Ezeani.[11a] This mechanism also involves a quadratic dependence of $k_A$ on [B] and the formation of a cyclic intermediate. The

authors found that in non-polar aprotic solvents nucleophilic aromatic substitution involving primary amines and substrates with fairly poor leaving groups will proceed predominantly by a catalyzed path through a cyclic transition state involving an eight-membered ring. This structure is formed through a network of the inter-hydrogen bonding between the zwitterionic intermediate and two amine molecules. A simplified scheme of this mechanism is shown in Scheme 2(c). The first step involves the formation of ZH. This intermediate reacts with two amine molecules to yield the eight-membered cyclic intermediate [$SB_3$], which evolves to products. The resulting expression for $k_A$ is

$$k_A = \frac{k_1 k_2 [B] + k_1 k_3 [B]^2}{k_{-1} + k_2 + k_3 [B]} \quad (9)$$

In reactions of amines with poor nucleofuges, the second step is usually rate determining so $k_{-1} \gg k_2 + k_3$ $[B]^2$ and the above expression simplifies to

$$k_A = k_1 k_2 / k_{-1} + k_1 k_3 / k_{-1} [B]^2 \quad (10)$$

showing a linear dependence between $k_A$ and the square of the nucleophile concentration. The intercept and the slope represent the non-catalytic and the catalytic rate coefficient, respectively. Banjoko and Ezeani[11a] found that whereas plots of $k_A$ vs amine concentration render straight lines with negative intercepts, plots of $k_A$ vs the square of the nucleophile concentration give rise to straight lines with positive intercepts. For reactions involving good leaving groups, the authors observed that the mechanism proceeds through a six-membered cyclic intermediate formed by a similar inter-hydrogen bonding between the zwitterionic intermediate and only one amine molecule.

For all the nucleophiles explored in the present work and over the whole range of amine concentrations, $k_A$ values do not exhibit a linear dependence with $[B]^2$ whereas plots of $k_A$ vs [B] do not afford lines with definite negative intercepts. These results and those corresponding to the evaluation of the dimer mechanism allow us to reject a quadratic dependence of $k_A$ on [B].

The six-membered cyclic transition state mechanism: the occurrence of a six-membered cyclic transition state was first proposed by Capon and Rees.[8a] As mentioned above, this transition state includes two molecules of amine which are joined through hydrogen bonds. The second molecule of amine may act as a proton donor to the leaving group as well as a proton acceptor from the positively charged nitrogen atom of the zwitterionic intermediate, the reaction to product taking place in a concerted manner. Ayediran *et al.*,[9a] considering the strength and the range of electrostatic forces in solvents of low ionizing power, proposed modifications for the base-catalyzed path: (i) the initial formation of a suitably

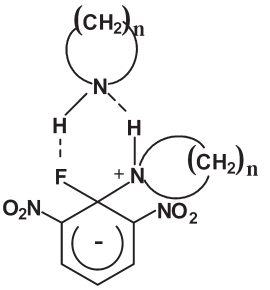


**Figure 5.** Six-membered cyclic intermediate structure

orientated dipolar aggregate between the zwitterionic intermediate and the nucleophile and (ii) when the nucleophile is a secondary amine, the breaking of the hydrogen bond with the *ortho*-nitro group will occur within the aggregate followed by proton exchange and the electrophilically catalyzed breaking of the C—F bond, i.e. it can be considered that the SB–GA mechanism takes place within the aggregate. Notwithstanding what the evolution to products is like, whether it proceed in a concerted or non-concerted way, the basic steps for this mechanism are illustrated in Scheme 2(d). The first step involves the formation of ZH. This intermediate reacts with another amine molecule to yield the six-membered cyclic intermediate [$SB_2$], which evolves to products. The proposed structure for this intermediate is shown in Fig. 5. This mechanism[8] generally exhibits total third-order reactions showing a linear relationship between $k_A$ values and initial amine concentration with negligible intercepts. The resulting $k_A$ expression would be $k_A = k_1 k_2 / k_{-1} + k_1 K_3 k_4 / k_{-1}$ [B].

The experimental evidence emerging from the present reactive systems which strongly support this latter mechanism is the following:

- The reactions show a second-order dependence on amine concentration and total third-order, exhibiting a linear relationship between the $k_A$ values and the initial amine concentration with negligible intercepts.
- The decomposition of the zwitterionic intermediate is the rate-determining step. The low activation enthalpies and the apparent absence of activation energy indicate that the reaction occurs stepwise; the rate-determining step must be preceded by at least one fast equilibrium, whereby the expected increase in rate for the slow step with increasing temperature would be compensated by a shift of the preceding equilibrium toward the reagents. The negative activation enthalpies require the exothermic formation of a weak complex preceding the rate-determining step.
- The reactions exhibit large negative values of the activation entropies, which corresponds to the formation of that aggregate or complex. This kind of mechanism was found for reactions carried out in solvents with low ionizing power, with low dipolarity/polarizability values, such as isooctane and hexane, and also

in solvents characterized by moderate values such as benzene and ethyl acetate. In this work, we extended the operability of this mechanism to EAc–$CHCl_3$ binary solvent mixtures in the EAc-rich zone.
- The extent of the influence of increasing temperature on reaction rates is related to the stability of that weak complex. The more stable the complex, the greater its equilibrium constant of formation. Therefore, an increase in temperature leads to an enhancement shift towards reactants and in this way to a decrease in the reaction rate. In connection with our experimental results, we assume that the corresponding complex with PYR would be less stable in comparison with those with PIP and HPIP, taking into account the fact that reactions with the former amine are less affected by the increasing temperature.

**Six-membered intermediate complex: theoretical calculations.** Semi-empirical molecular orbital calculations were performed in order to obtain a relative stability order of the proposed intermediate complex. In this direction, the complex intermediate structures for PYR, PIP and HPIP were optimized at the AM1 level.[12] In order to perform these calculations, the corresponding results obtained in previous work[1b] for the structures of each amine and for each ZH were taken into account. Figures S9, S10 and S11 (ESI) show the optimized structures which represent a local minimum in the potential energy surface for the complexes with PYR, PIP and HPIP, respectively. Table 5 presents the total energy ($E_T$), the heat of formation ($\Delta H^{\#}$), the heat of formation with respect to reactants ($\Delta\Delta H^{\#}$) of the respective complexes and the inter-atomic distances between the ammonium hydrogen of ZH and the nitrogen atom of the entering amine ($D_{N-H}$) and between the fluorine atom of ZH and the hydrogen (amino group) of the amine ($D_{F-H}$). These values correspond to four different optimized structures, obtained by perturbing the system and allowing it to evolve to the respective geometry.

The results allow us to make the following remarks:

- The negative $\Delta\Delta H^{\#}$ values indicate that the formation of these complexes is exothermic and that they constitute stable structures.
- The complex with PYR is the structure with the highest energy and is less stable than the corresponding complexes with PIP and HPIP, thus verifying what we expressed in the paragraphs above.
- The magnitudes of the $D_{N-H}$ and $D_{F-H}$ inter-atomic distances suggest that the interaction forces coming into play are electrostatic rather than hydrogen-bond type.[13] This result favors the formation of a suitably orientated dipolar aggregate rather than an inter-hydrogen bonding structure.

## CONCLUSIONS

Based on the overall evaluation presented in this paper, we can conclude the following: (i) the analysis of Arrhenius lines allowed us to prove the existence of isokinetic relationships, which were used as a diagnostic tool in order to infer a changeover in the nature of the rate-determining transition state as a function of solvent composition; (ii) the reactions with the explored secondary amines carried out in pure EAc and EAc–$CHCl_3$ solvent mixtures at $X_{CoS} = 0.1$, and in some cases also at $X_{CoS} = 0.3$, proceed via the formation of a six-membered orientated dipolar aggregate in which the SB–GA mechanism may take place; (iii) the reactions carried out in the remaining solvent mixtures evolve towards the classical SB–GA mechanism.

**Table 5.** Total energy, heats of formation and inter-atomic distances at the AM1 level corresponding to the different complexes[a]

| Complex | $E_T$ (kJ mol$^{-1}$) | $\Delta H^{\#}$ (kJ mol$^{-1}$) | $\Delta\Delta H^{\#}$ (kJ mol$^{-1}$) | $D_{N-H}$ (Å) | $D_{F-H}$ (Å) |
|---|---|---|---|---|---|
| 2,6-DNFB + PYR | | | | | |
| 1 | −450766.1 | −51.59 | −90.29 | 2.74734 | 2.34827 |
| 2 | −450766.1 | −51.60 | −90.29 | 2.71905 | 2.38004 |
| 3 | −450766.1 | −51.60 | −90.33 | 2.71585 | 2.37614 |
| 4 | −450766.1 | 51.60 | −90.33 | 2.71917 | 2.37768 |
| 2,6-DNFB + PIP | | | | | |
| 1 | −480888.5 | −145.1 | −136.9 | 2.58408 | 2.40092 |
| 2 | −480888.5 | −145.0 | −136.7 | 2.61162 | 2.48852 |
| 3 | −480888.5 | −145.0 | −136.7 | 2.62010 | 2.49330 |
| 4 | −480888.5 | −145.1 | −136.9 | 2.58744 | 2.38766 |
| 2,6-DNFB + HPIP | | | | | |
| 1 | −510944.0 | −171.3 | −149.3 | 2.74540 | 2.41476 |
| 2 | −510943.6 | −171.1 | −149.1 | 2.800868 | 2.35458 |
| 3 | −510944.0 | −171.3 | −149.3 | 2.75368 | 2.40743 |
| 4 | −510944.0 | −171.3 | −149.3 | 2.76642 | 2.40271 |

[a] $E_T$ = total energy; $\Delta H^{\#}$ = heat of formation; $\Delta\Delta H^{\#}$ = heat of formation with respect to reactants; $D_{N-H}$ and $D_{F-H}$ = inter-atomic distances.

## EXPERIMENTAL

2,6-DNFB was synthesized as reported previously.[14] PYR, PIP, HPIP and the corresponding solvents were purified as usual.[15] The solvents were kept over 4 Å molecular sieves and stored in special vessels that allow delivery without air contamination. All binary mixtures were prepared prior to use. $\Delta H^{\#}$ and $\Delta S^{\#}$ were calculated by means of the Eyring equation. The $\Delta G^{\#}$ values were calculated from $\Delta H^{\#}$ and $\Delta S^{\#}$ values at 25 °C. $T_{hm}$ was close to 25 °C so that this temperature was selected as the harmonic mean temperature.

The kinetics of the reactions were studied by UV–visible spectrophotometry. A Perkin-Elmer Model 124 spectrophotometer was used, equipped with a data acquisition system. Molecular orbital calculations were carried out using the HyperChem 5.11 system of programs. Computational details are presented in the Electronic Supplementary Information.

### Acknowledgements

We are indebted to the Universidad Nacional del Litoral (UNL), República Argentina. This work received financial support from the Science and Technology Secretariat, UNL, CAI + D Program (Projects 2000-17-151, 2002-21-152 and 2002-21-153).

## REFERENCES

1. (a) Mancini PM, Fortunato GG, Adam C, Vottero LR, Terenzani AJ. *J. Phys. Org. Chem.* 2002; **15**: 258–269; (b) Mancini PM, Fortunato GG, Vottero LR. *J. Phys. Org. Chem.* 2004; **17**: 138–147.
2. (a) Orvick JA, Bunnett JF. *J. Am. Chem. Soc.* 1970; **92**: 2417–2427; (b) Bunnett JF, Sekiguchi S, Smith LA. *J. Am. Chem. Soc.* 1981; **103**: 4865–4871; (c) Nudelman NS, Mancini PME, Martinez RD, Vottero LR. *J. Chem. Soc., Perkin Trans 2* 1987; 951–954; (d) Sekiguchi S, Hosokawa M, Suzuki T, Sato M. *J. Chem. Soc., Perkin Trans 2* 1993; 1111–1118.
3. Linert W. *Chem. Soc. Rev.* 1994; 429–438.
4. Linert W. *Inorg. Chim. Acta* 1988; **141**: 233–242.
5. Krug R. *Ind. Eng. Chem. Fundam.* 1980; **19**: 50–59.
6. (a) Bunnett J. In *Techniques of Chemistry*, vol. 6, Lewis ES (ed). Wiley: New York, 1974 Chapt. VIII; (b) Bernasconi C, Zollinger H. *Helv. Chim. Acta* 1966; **49**: 103–111.
7. (a) Forlani L. *J. Chem. Res. (S)* 1984; **66**: 260–261; (b) Forlani L, Todesco PE. *J. Chem. Soc., Perkin Trans. 2* 1988; 1585–1589; (c) Chiacchiera SM, Singh JO, Anunziata JD, Silber JJ. *J. Chem. Soc., Perkin Trans. 2* 1988; 1585–1589; (d) Durantini E, Zingaretti JD, Anunziata JD, Silber JJ. *J. Phys. Org. Chem.* 1992; **5**: 557–565.
8. (a) Capon B, Rees W. *Annu. Rep. Prog. Chem.* 1963; 247–293; (b) Bitter B, Zollinger H. *Helv. Chim. Acta* 1961; **44**: 812–823; (c) Illuminatti G, La Torre F, Liggieri G, Sleiter G, Stegel F. *J. Am. Chem. Soc.* 1975; **97**: 1851–1854.
9. (a) Ayediran T, Bamkole O, Hirst J, Onyido I. *J. Chem. Soc., Perkin Trans. 2* 1977; 597–600; (b) Bamkole O, Hirst J, Onyido I. *J. Chem. Soc., Perkin Trans. 2* 1982; 889–893.
10. (a) Nudelman NS, Palleros D. *J. Org. Chem.* 1989; **2**: 1607–1612; (b) Nudelman NS. In *The Chemistry of Amino, Nitroso, Nitro and Related groups*, Patai S (ed). Wiley: Chichester, 1996; Chapt. 26.
11. (a) Banjoko O, Ezeani J. *J. Chem. Soc., Perkin Trans. 2* 1982; 1357–1360; (b) Banjoko O, Ezeani J. *J. Chem. Soc., Perkin Trans. 2* 1986; 531–536; (c) Banjoko O, Bayeroju YA. *J. Chem. Soc., Perkin Trans. 2* 1988; 1853–1857.
12. (a) Dewar MJS, Zoebisch EG, Healy EF, Stewart JJP. *J. Am. Chem. Soc.* 1985; **107**: 3902–3909; (b) Dewar MJS, Dieter KM. *J. Am. Chem. Soc*. 1886; **108**: 8075–8086; (c) Stewart JJP. *J. Comput. Aided. Mol. Des.* 1990; **4**: 1–105.
13. Jeffrey GA. *An Introduction to Hydrogen Bonding*. Oxford University Press: Oxford, 1997; 11–16.
14. Parker RE, Read TO. *J. Chem. Soc*. 1962; 3149–3153.
15. (a) Mancini PM, Terenzani AJ, Adam C, Pérez A, Vottero LR. *J. Phys. Org. Chem.* 1999; **12**: 713–724; (b) Mancini PM, Terenzani AJ, Adam C, Pérez A, Vottero LR. *J. Phys. Org. Chem.* 1999; **12**: 207–220; (c) Mancini PM, Adam C, Pérez A, Vottero LR. *J. Phys. Org. Chem.* 2000; **13**: 221–231.

 